

Supporting Information

Biotinylated and fluorophore-incorporated polymeric mixed micelles for tumor cell-specific turn-on fluorescence imaging of Al³⁺

Cai-Xia Wang,^a Shu-Lun Ai,^b Bo Wu,^b Shi-Wen Huang,^{*b} Zhihong Liu^{*a}

*^aHubei Collaborative Innovation Center for Advanced Organic Chemical Materials,
Ministry of Education Key Laboratory for the Synthesis and Application of Organic
Functional Molecules and College of Chemistry and Chemical Engineering, Hubei
University, Wuhan 430062, P. R. China.*

*^bKey Laboratory of Biomedical Polymers (Ministry of Education), College of
Chemistry and Molecular Sciences, Wuhan University, Wuhan 430072, P. R. China.*

*Corresponding author.

E-mail address: zhliu@whu.edu.cn; swhuang@whu.edu.cn

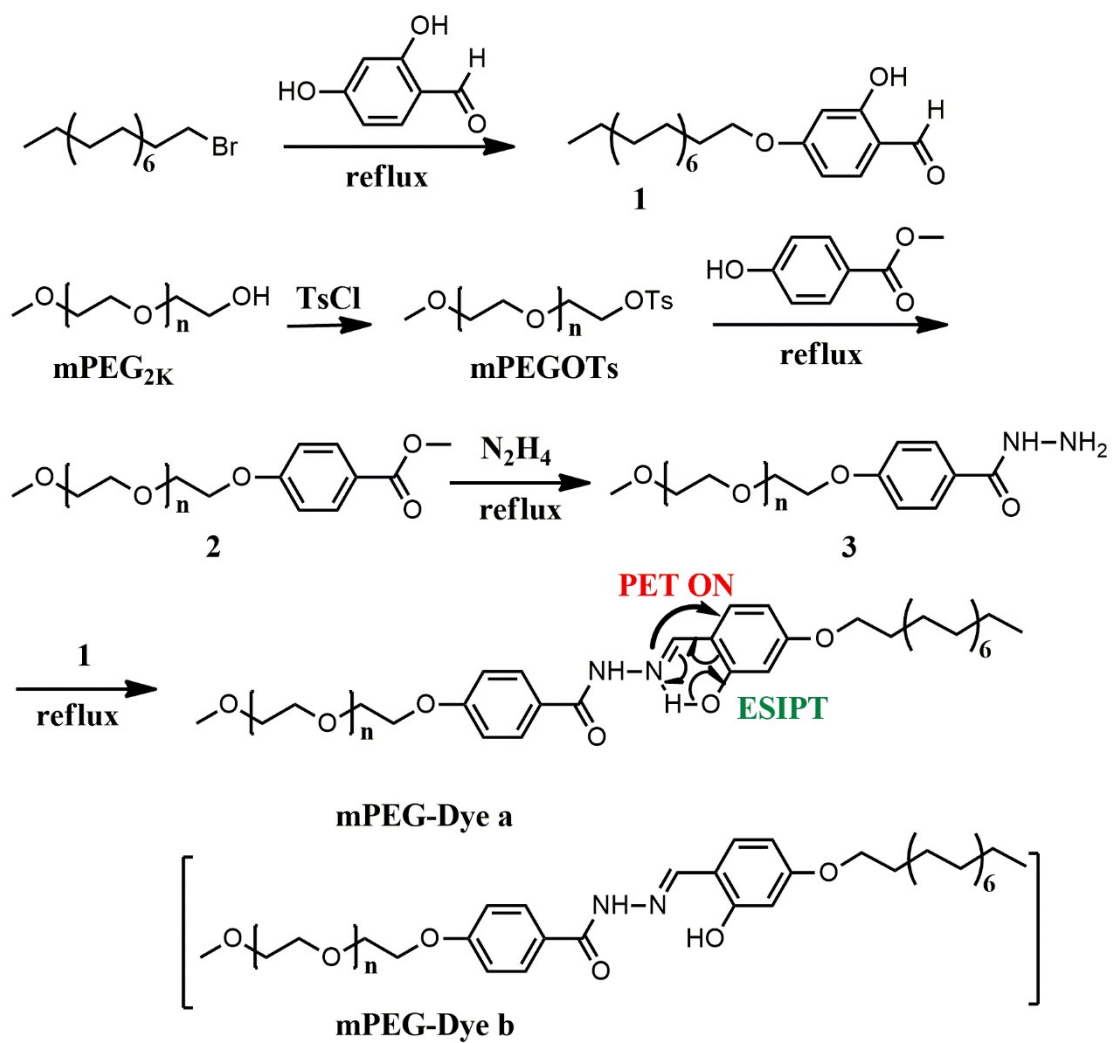


Figure S1. Synthesis of mPEG-Dye.

The structural characterization of compound 1

$^1\text{H NMR}$ (CDCl_3 , 400 MHz): δ 11.486 (s, H_a), 9.706 (s, H_b), 7.43 (d, H_c), 6.545 (d, H_d), 6.416 (s, H_e), 4.003 (t, 2 H_f), 1.793 (t, 2 H_g), 1.585 (d, 2 H_h), 1.447-1.259 (m, 24 H_i), 0.88 (d, 3 H_j).

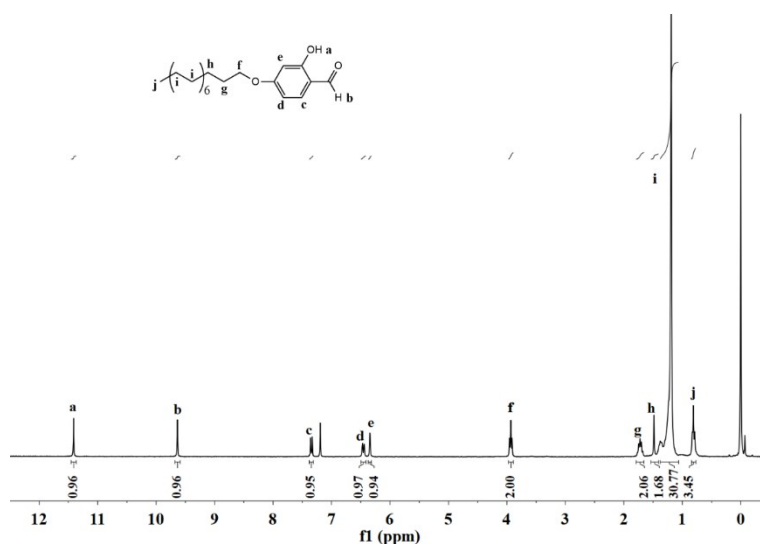


Figure S2. $^1\text{H NMR}$ spectrum of compound 1 in CDCl_3 .

The structural characterization of compound 2

$^1\text{H NMR}$ (DMSO-d_6 , 400 MHz): δ 7.90 (d, 2 H_a), 7.054 (d, 2 H_b), 4.157 (t, 2 H_c), 3.792 (s, 3 H_d), 3.738 (t, 2 H_e), 3.486-3.421 (m, 176 H_f), 3.247 (s, 3 H_g).

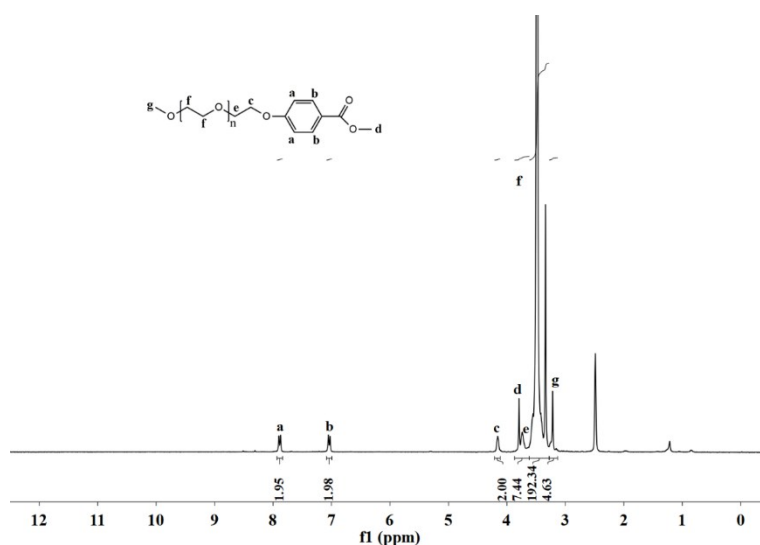


Figure S3. $^1\text{H NMR}$ spectrum of compound 2 in deuterated DMSO.

^1H NMR (CDCl_3 , 400 MHz): δ 7.907 (d, 2H_a), 6.866 (d, 2H_b), 4.117 (t, 2H_c), 3.81 (s, 3H_d), 3.746 (t, 2H_e), 3.646 -3.487 (m, 176H_f), 3.313 (s, 3H_g).

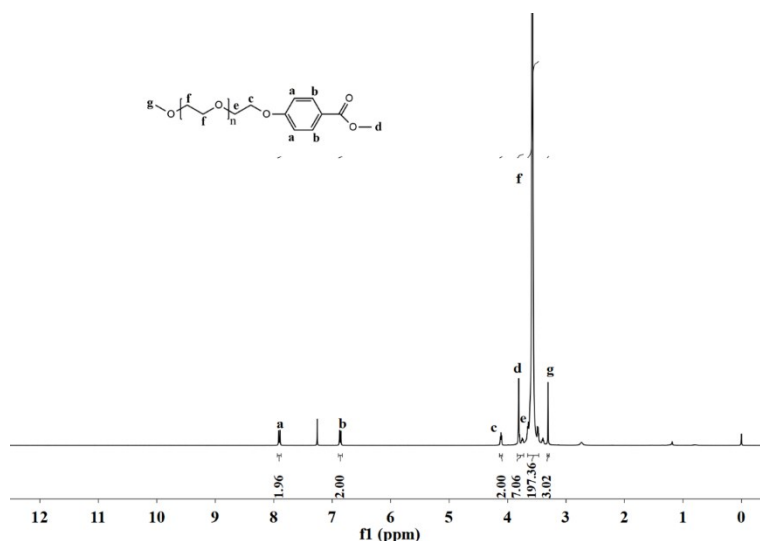


Figure S4. ^1H NMR spectrum of compound **2** in CDCl_3 .

The structural characterization of compound **3**

^1H NMR (DMSO-d_6 , 400 MHz): δ 9.622 (t, H_a), 7.799 (d, 2H_b), 6.997 (d, 2H_c), 4.157 (d, 2H_d), 4.134 (t, 2H_e), 3.742 (t, 2H_f), 3.505 -3.43 (m, 176H_g), 3.235 (s, 3H_h), 1.234 (s, H_2O).

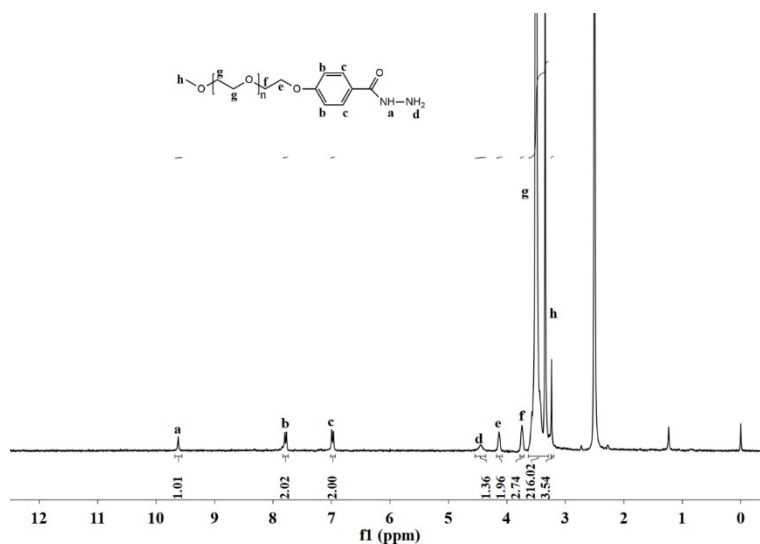


Figure S5. ^1H NMR spectrum of compound **3** in deuterated DMSO .

^1H NMR (CDCl_3 , 400 MHz): 7.762 (d, 2H_b), 6.942 (d, 2H_c), 4.163 (d, 2H_e), 3.846 (t, 2H_f), 3.689 -3.523 (m, 176H_g), 3.355 (s, 3H_h), 1.228 (s, H_2O).

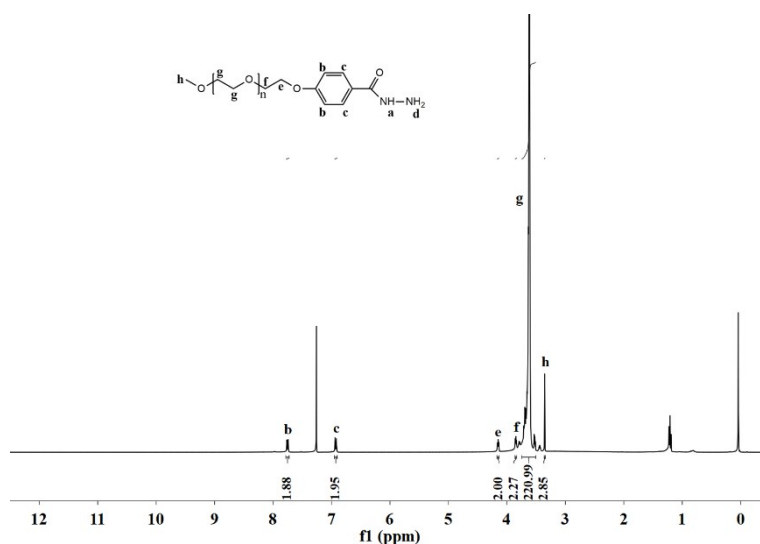


Figure S6. ^1H NMR spectrum of compound **3** in CDCl_3 .

The structural characterization of the polymer mPEG-Dye

Isomer a: ^1H NMR (DMSO-d_6 , 400 MHz): δ 11.888 (s, H_1), 8.514 (s, H_2), 7.916 (d, 2H_3), 7.398 (d, H_4), 7.099 (d, 2H_5), 6.517 (m, H_6 , H_7), 4.18 (t, 2H_8), 3.973 (t, 2H_9), 3.771 (t, 2H_{10}), 3.582-3.501 (m, 176H_{11}), 3.232 (s, 3H_{12}), 1.693 (m, 2H_{13}), 1.40 -1.232 (m, 26H_{14}), 0.845 (t, 3H_{15})

Isomer b: ^1H NMR (DMSO-d_6 , 400 MHz): δ 11.689 (s, H_1), 8.319 (s, H_2), 7.892 (d, 2H_3), 7.369 (d, H_4), 7.070 (d, 2H_5), 6.468 (m, H_6 , H_7), 4.18 (t, 2H_8), 3.973 (t, 2H_9), 3.771 (t, 2H_{10}), 3.582-3.501 (m, 176H_{11}), 3.232 (s, 3H_{12}), 1.693 (m, 2H_{13}), 1.40 -1.232 (m, 26H_{14}), 0.845 (t, 3H_{15})

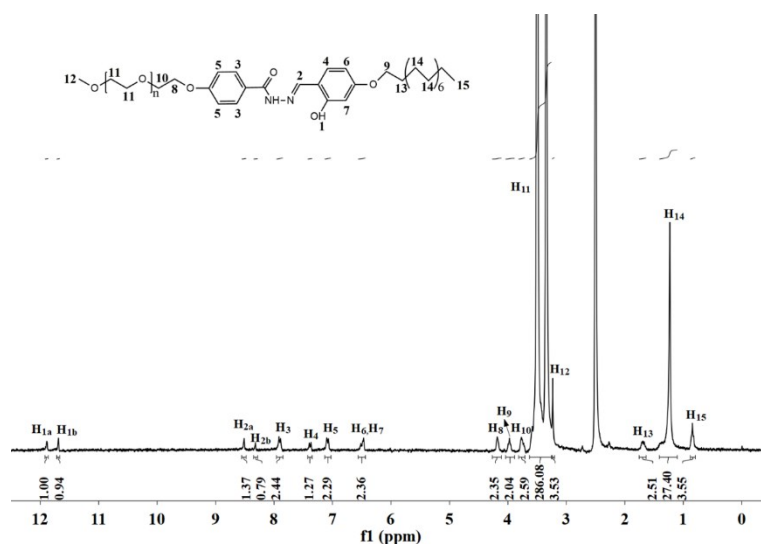


Figure S7. ^1H NMR spectrum of polymer mPEG-Dye in deuterated DMSO.

^1H NMR (CDCl_3 , 400 MHz): δ 8.409 (s, H_2), 7.821(d, 2H_3), 7.303(d, H_4), 6.945(d, 2H_5), 6.513(m, H_6 , H_7), 4.178(t, 2H_8), 3.937(t, 2H_9), 3.861 (t, 2H_{10}), 3.702-3.537 (m, 176H_{11}), 3.366 (s, 3H_{12}), 1.738 (m, 2H_{13}), 1.429 -1.241 (m, 26H_{14}), 0.862 (t, 3H_{15})

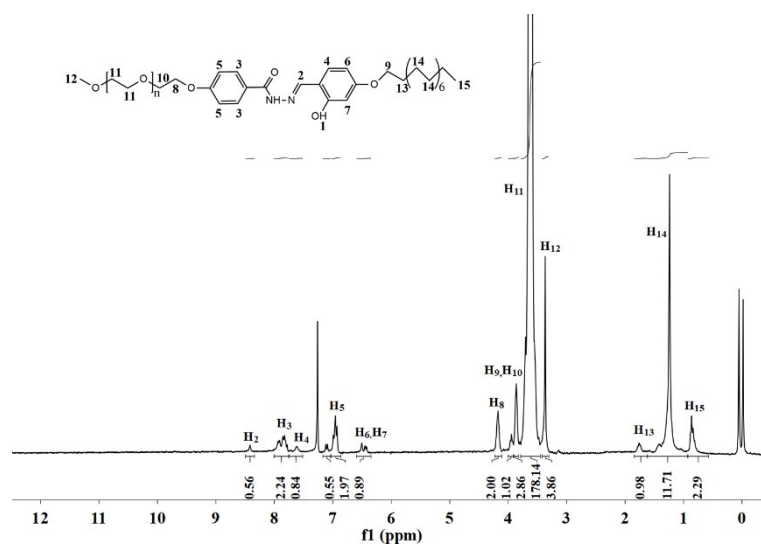


Figure S8. ^1H NMR spectrum of polymer mPEG-Dye in CDCl_3 .

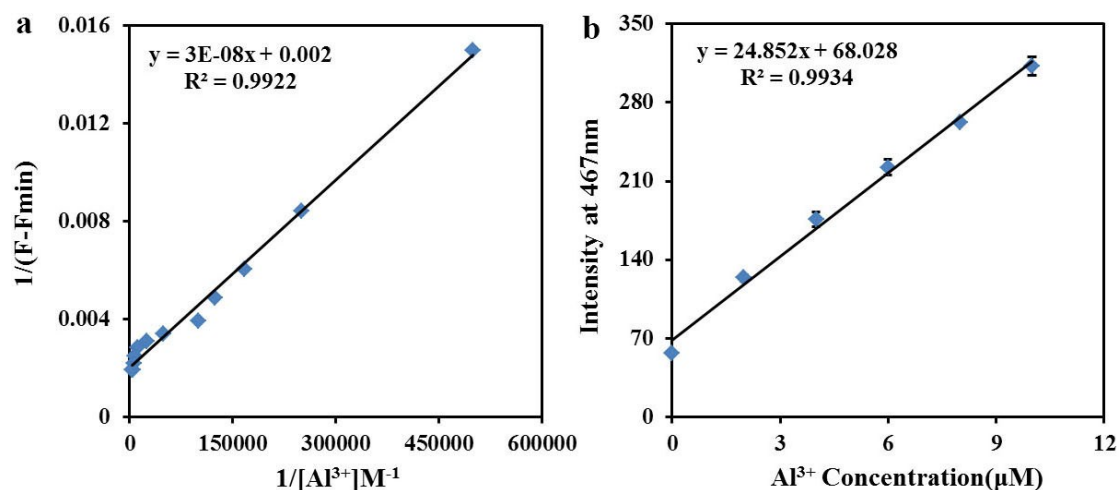


Figure S9. (a) Benesi-Hildebrand analysis of the emission changes for the complexation between mPEG-Dye and Al^{3+} . (b) Linear fluorescence enhancement of mPEG-Dye (20 μM) response to Al^{3+} concentration (0-10 μM).

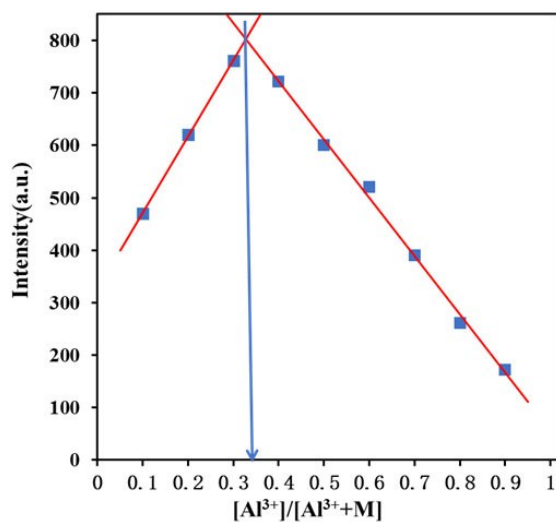


Figure S10. Job's plots for determining the stoichiometry of mPEG-Dye (M) and Al^{3+} in H_2O . The total concentration of mPEG-Dye and Al^{3+} was 20 μM ($\lambda_{ex} = 408$ nm, $\lambda_{em} = 467$ nm).

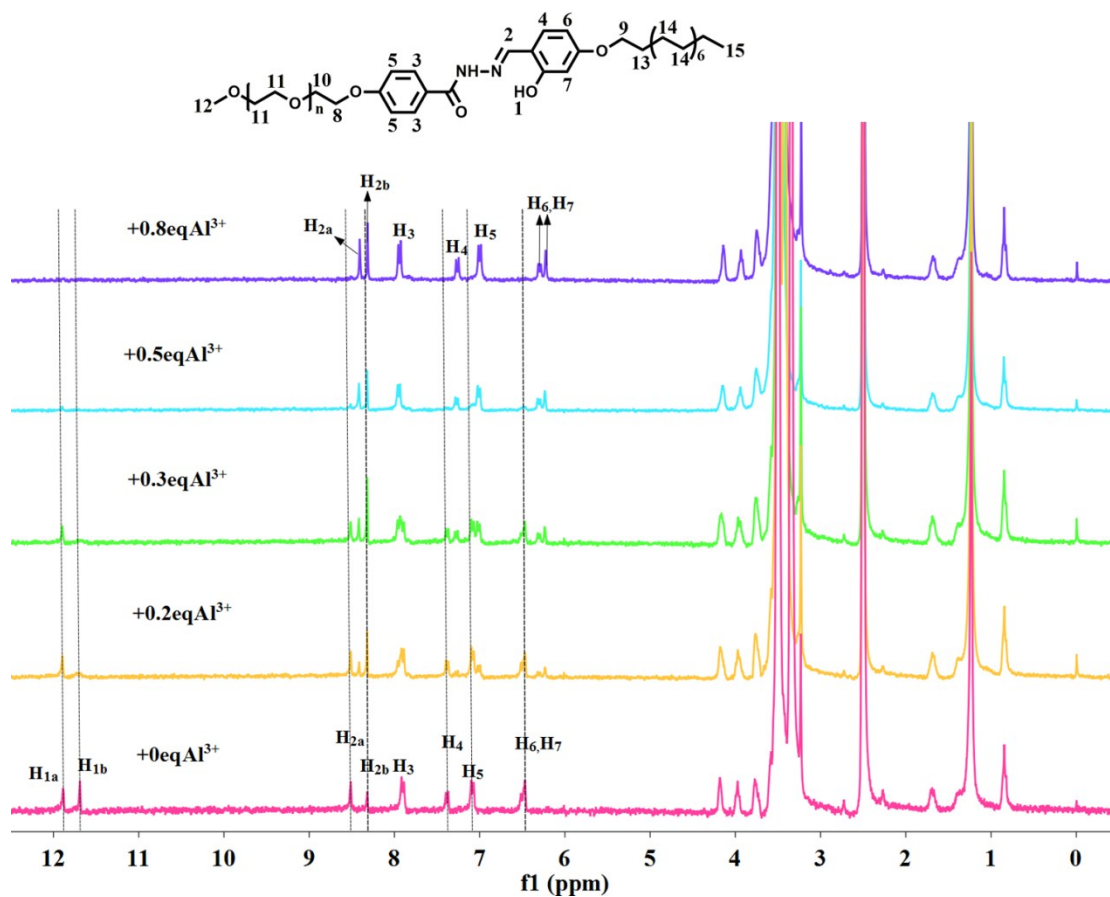


Figure S11. ^1H NMR of mPEG-Dye (10 mM) in DMSO-d_6 upon addition of various amount of Al^{3+} cation.

Table S1. Physicochemical properties of two micelles

Sample	TEM particle size(nm)	Hydrodynamic particle size(nm)	PDI
mPEG-Dye	15±3	18±0.05	0.213±0.01
mPEG-Dye-Biotin	18±3	21±0.04	0.201±0.01

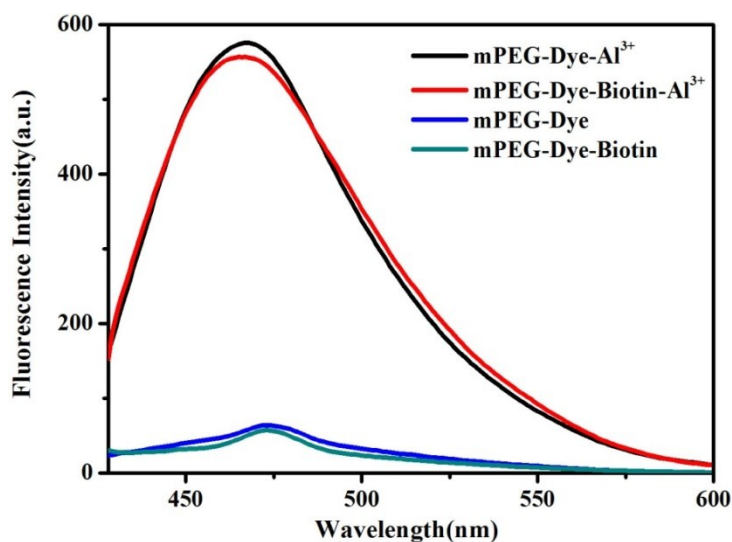


Figure S12. Fluorescence spectra of mPEG-Dye (20 μM) alone, mPEG-Dye-Biotin (20 μM) alone, mPEG-Dye (20 μM) with Al^{3+} (200 μM) and mPEG-Dye-Biotin (20 μM) with Al^{3+} (200 μM) in H_2O .

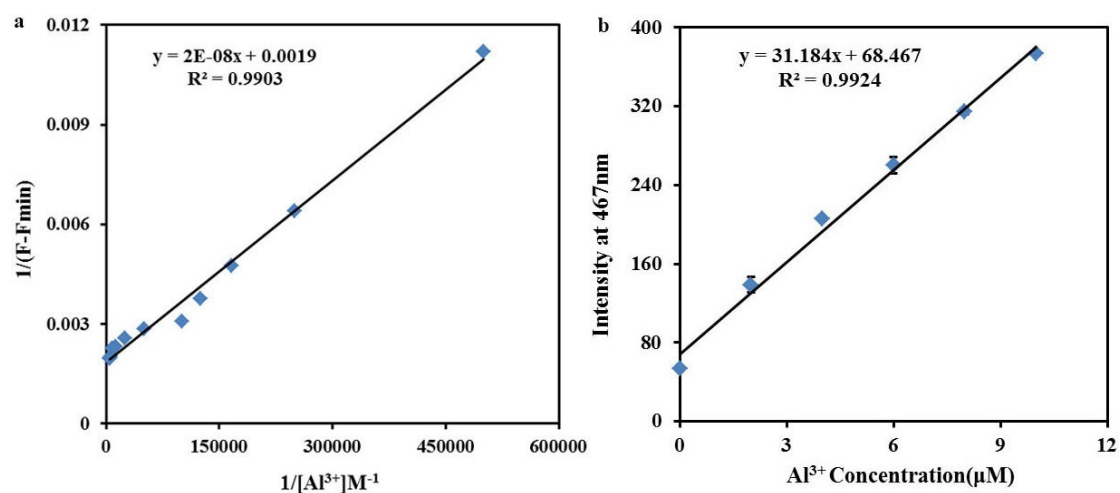


Figure S13. (a) Benesi-Hildebrand analysis of the emission changes for the complexation between mPEG-Dye-Biotin and Al^{3+} . (b) Linear fluorescence enhancement of mPEG-Dye-Biotin (20 μM) response to Al^{3+} concentration (0-10 μM).

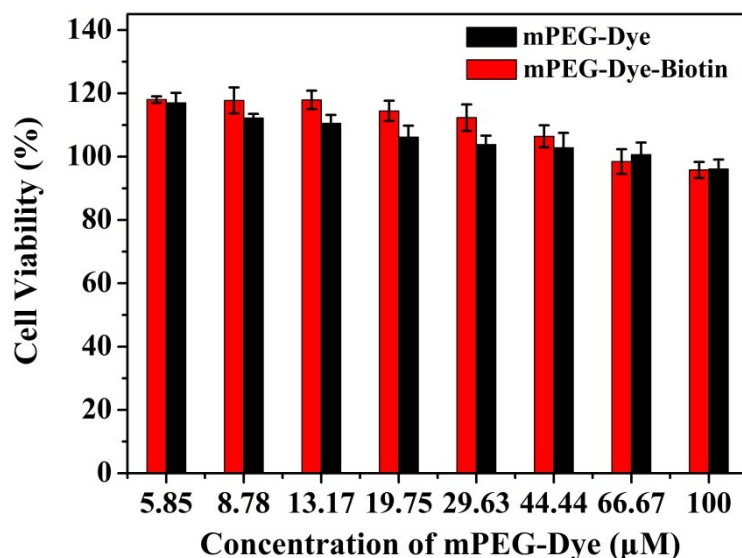


Figure S14. Cytotoxicity of mPEG-Dye-Biotin and mPEG-Dye against HeLa cells. Data are presented as \pm SD (n=4).

Table S2 Comparison of some schiff base probes for Al³⁺ detection.

Probe	Testing media	Association Constant (M ⁻¹)	Detection limit (M)	Imaging Al ³⁺ in live cells
Present work (mPEG-Dye-Biotin)	Aqueous solution	9.5×10^4	2.02×10^{-8}	Yes
Diarylethene-based fluorescent chemosensor (10) ¹	Acetonitrile	4.90×10^4	2.7×10^{-8}	No
Nitrogen heterocycle platform based fluorescence chemosensor(L) ²	Methanol	4.72×10^4	1.24×10^{-5}	No
Fluorene-based Schiff-base fluorescent chemosensor(F3) ³	CH ₃ CN	5.44×10^4	3.1×10^{-7}	No
Tetra(3-[benzoylhydrazone]-methyl-4-hydroxyphenyl) ethene (IV) ⁴	DMSO: H ₂ O (9:1, v/v)	9.44×10^2	5×10^{-7}	No
Oligothiophene-phenylamine-based fluorescence sensor (3TP) ⁵	THF: H ₂ O (7:3, v/v)	8.66×10^5	1.77×10^{-7}	No
2-amino-4,5-imidazole dicarbonyl nitrile and 8-hydroxy-julolidine-9-carboxaldehyde(1) ⁶	MeOH: H ₂ O (5:15, v/v)	2.7×10^3	3.44×10^{-6}	No
Fluorescence chemosensor based on rhodamine and azobenzene moieties(L) ⁷	C ₂ H ₅ OH:H ₂ O (4:1, v/v)	7.03×10^3	1.1×10^{-7}	No
Schiff base fluorescence probe (STH) ⁸	EtOH:H ₂ O (9:1, v/v)	6.74×10^3	1.07×10^{-6}	Yes
Unsymmetrical azine derivative (NDEA) ⁹	DMSO: H ₂ O: MeOH (0.1 : 1.9 : 8.0, v/v)	2.47×10^4	1.65×10^{-7}	Yes
Schiff base-type fluorescent chemosensor ¹⁰	Aqueous solution	7.80×10^4	0.17×10^{-6}	Yes

References

- 1 S. Wang, L. Ma, G. Liu and S. Pu, *Dyes Pigm.*, 2019, **164**, 257-266.
- 2 J. Lv, Y. Fu, G. Liu, C. Fan and S. Pu, *RSC Adv.*, 2019, **9**, 10395-10404.
- 3 M. Tajbakhsh, G. B. Chalmardi, A. Bekhradnia, R. Hosseinzadeh, N. Hasani and M. A. Amiri, *Spectrochim. Acta. A. Mol. Biomol. Spectrosc.*, 2018, **189**, 22-31.
- 4 F. Wang, X. Zeng, X. Zhao, H. Lu and Q. Wang, *J. Lumin.*, 2019, **208**, 302-306.
- 5 Z. Guo, Q. Niu and T. Li, *Spectrochim. Acta. A. Mol. Biomol. Spectrosc.*, 2018, **200**, 76-84.
- 6 S. Y. Kim, S. Y. Lee, J. H. Kang, M. S. Kim, A. Kim and C. Kim, *J. Coord. Chem.*, 2018, **71**, 2401-2414.
- 7 S. Chand, M. Mondal, S. C. Pal, A. Pal, S. Maji, D. Mandal and M. C. Das, *New J. Chem.*, 2018, **42**, 12865-12871.
- 8 Y. Zhu, X. Gong, Z. Li, X. Zhao, Z. Liu, D. Cao and R. Guan, *Spectrochim. Acta. A. Mol. Biomol. Spectrosc.*, 2019, **219**, 202-205.
- 9 R. Yadav, A. Rai, A. K. Sonkar, V. Rai, S. C. Gupta and L. Mishra, *New J. Chem.*, 2019, **43**, 7109-7119.
- 10 Y. Y. Guo, L. Z. Yang, J. X. Ru, X. Yao, J. Wu, W. Dou, W. W. Qin, G. L. Zhang, X. L. Tang and W. S. Liu, *Dyes Pigm.*, 2013, **99**, 693-698.